

# Microscopic Theory of Magnetic Detwinning in Iron-Based Superconductors with Large-Spin Rare Earths

Jannis Maiwald, I. I. Mazin, Philipp Gegenwart

## Angaben zur Veröffentlichung / Publication details:

Maiwald, Jannis, I. I. Mazin, and Philipp Gegenwart. 2018. "Microscopic Theory of Magnetic Detwinning in Iron-Based Superconductors with Large-Spin Rare Earths." *Physical Review X* 8 (1): 011011-1-011011-9.  
<https://doi.org/10.1103/PhysRevX.8.011011>.

# Microscopic Theory of Magnetic Detwinning in Iron-Based Superconductors with Large-Spin Rare Earths

Jannis Maiwald,<sup>1</sup> I. I. Mazin,<sup>2</sup> and Philipp Gegenwart<sup>1</sup>

<sup>1</sup>*Experimentalphysik VI, Universität Augsburg, Universitätsstraße 1, 86135 Augsburg, Germany*

<sup>2</sup>*Code 6393, Naval Research Laboratory, Washington, DC 20375, USA*

 (Received 10 June 2017; revised manuscript received 8 December 2017; published 23 January 2018)

Detwinning of magnetic (nematic) domains in Fe-based superconductors has so far only been obtained through mechanical straining, which considerably perturbs the ground state of these materials. The recently discovered nonmechanical detwinning in  $\text{EuFe}_2\text{As}_2$  by ultralow magnetic fields offers an entirely different, nonperturbing way to achieve the same goal. However, this way seemed risky due to the lack of a microscopic understanding of the magnetically driven detwinning. Specifically, the following issues remained unexplained: (i) ultralow value of the first detwinning field of approximately 0.1 T, two orders of magnitude below that of  $\text{BaFe}_2\text{As}_2$ , and (ii) reversal of the preferential domain orientation at approximately 1 T and restoration of the low-field orientation above 10–15 T. In this paper, we present, using published as well as newly measured data, a full theory that quantitatively explains all the observations. The key ingredient of this theory is a biquadratic coupling between Fe and Eu spins, analogous to the Fe-Fe biquadratic coupling that drives the nematic transition in this family of materials.

DOI: [10.1103/PhysRevX.8.011011](https://doi.org/10.1103/PhysRevX.8.011011)

Subject Areas: Condensed Matter Physics, Magnetism, Materials Science, Superconductivity

## I. INTRODUCTION

One of the most admirable experimental feats in studies of Fe-based superconductors (FeBS) is the mechanical detwinning of the low-temperature phases of the parent compounds in the 122 families [1,2]. This allowed impressive insight into the physics of spin-driven nematicity, a phenomenon that arguably rivals the superconductivity itself in these materials. In this connection, one of the most intriguing and unexpected findings was that this nematic physics is ensured by a sizable biquadratic magnetic interaction, something unheard of in localized magnetic moment systems and never investigated in itinerant magnetic metals. This phenomenon was first discovered computationally [3] and later shown to provide the only physically meaningful description of spin dynamics in FeBS [4]. There is growing evidence that it is not limited to FeBS, but occurs also in other itinerant systems [5].

Mechanical straining is not the only way to detwin FeBS. It was shown that a static magnetic field of approximately 15 T leads to partial detwinning [6] and pulsed fields of approximately 30 T to nearly complete detwinning [7].

Later, we will analyze these facts in more detail, but at the moment we emphasize that these are relatively large fields, even though the in-plane magnetic anisotropy energy of the FeAs planes was experimentally shown to be of the order of 0.5 meV and, therefore, sizable compared to, e.g., elemental Fe, where it is only a few  $\mu\text{eV}$ . Against this background, it came as a complete surprise when it was discovered [8,9] that substituting Ba with Eu lowers the field needed for full detwinning by two orders of magnitude. In principle, this magnetic detwinning allows for a virtually nonintrusive (the energy scale associated with this field is less than 20 mK) investigation of the physics of the nematic state. However, this seemingly exciting opportunity was met with limited enthusiasm for the simple reason that no plausible microscopic explanation could be found for the detwinning itself, given the minuscule amplitude of the required field. Even more striking was the discovery that by increasing the magnetic field gradually one can switch the sign of detwinning *twice*: initially, twin domains orient in such a way that the Fe-Fe ferromagnetic bonds along the crystallographic  $b$  are parallel to the applied field [we call this the “b-twin”; see Fig. 1(a)]. This process is essentially complete at  $H_0 \sim 0.5$  T. Then, at  $H_1 \sim 1$  T, domains spontaneously rotate in-plane by  $90^\circ$ , and at  $H_2 \sim 10$  T, they start to turn back to the detwinned state that was initially generated at  $H \lesssim 0.5$  T; see also Figs. 1(b)–1(h). With such a complex phase diagram, and no theoretical understanding of the underlying phenomena, it is indeed

---

*Published by the American Physical Society under the terms of the Creative Commons Attribution 4.0 International license. Further distribution of this work must maintain attribution to the author(s) and the published article's title, journal citation, and DOI.*

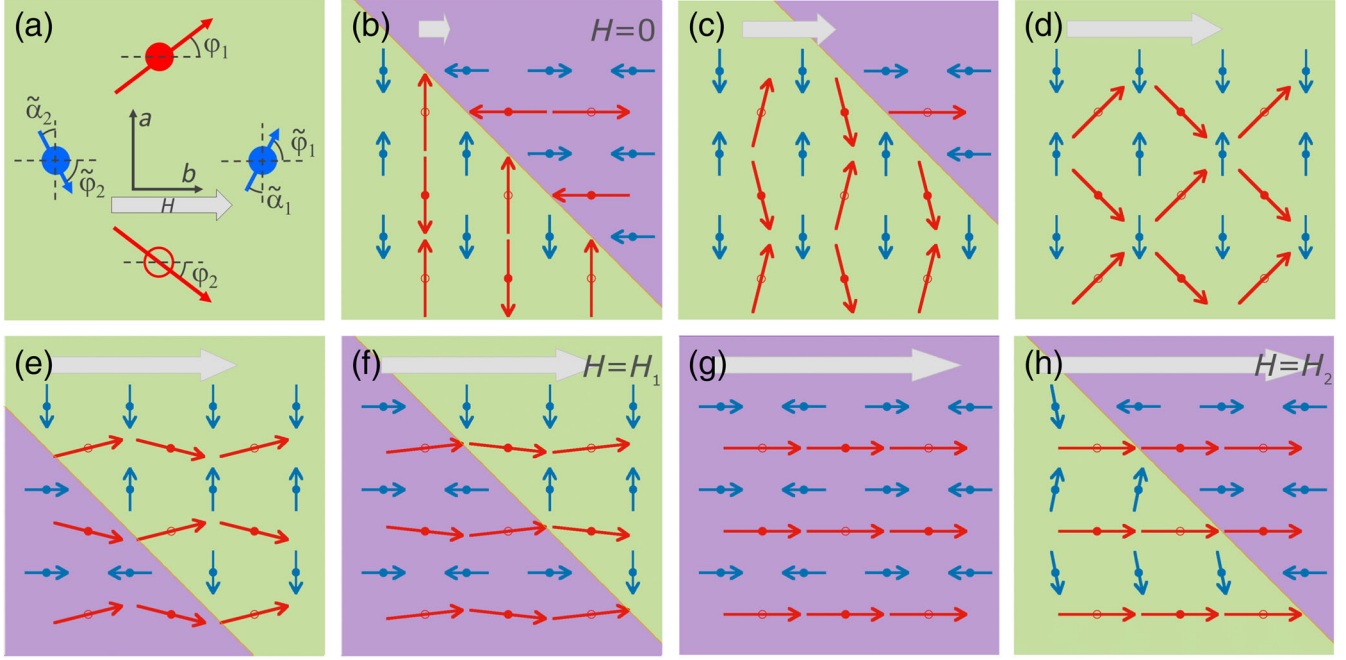


FIG. 1. Low-temperature kinetic detwinning process of  $\text{EuFe}_2\text{As}_2$  for an increasing (from left to right) external magnetic field  $H\parallel[110]_{\text{T}}$  (gray arrows). Fe atoms and spins are shown in blue. Open circles indicate Eu atoms and spins (red) in the next layer. (a) Definition of the spin angles. (b) Initial twin population (a b-twin domain in green, an a-twin one in purple) at  $H = 0$ . (c) The b-twin domains grow with increasing field until (d) the system is completely detwinned, and only b-twin domains ( $b\parallel H$ ) are present. (e) Above  $H_0$ , the first reorientation sets in, and the population of the a-twin domains starts to grow. (f) At  $H_1$  the two populations are equal. (g) At a higher field, the system becomes again fully detwinned ( $a\parallel H$ , no more b-twin domains). (h) At an even higher field, another reorientation starts, and at  $H_2$ , the populations of the two domain types are equal again (at even higher fields, eventually the b-twin domains will dominate).

worrisome to embark on systematic studies of nematicity with the risk that unknown magnetic physics may affect the findings. The goal of this paper is to remedy this situation and present a full and quantitative theory explaining all the above observations. It appears that magnetically induced detwinning is intimately related to the nature of nematicity itself; namely, it is also driven by a sizable biquadratic interaction, which, in turn, is the consequence of the Janusian itinerant-localized nature of the FeBS.

## II. FORMALISM

We start with the (simpler) case of  $\text{BaFe}_2\text{As}_2$ . The minimal approximation is the nearest-neighbor (n.n) Heisenberg model with single-site anisotropy:

$$\mathcal{H}_{\text{Fe}} = -\tilde{D} \sum_i f_{i,a}^2 + \tilde{J} \sum_{\langle ij \rangle} \mathbf{f}_i \cdot \mathbf{f}_j - \tilde{M} \sum_i \mathbf{f}_i \cdot \mathbf{H}, \quad (1)$$

where  $i, j$  label Fe sites;  $\mathbf{f}_i$  is the unit vector directed along the Fe magnetic moment at site  $i$ ;  $\tilde{M}$  is its absolute value; and the summation is over all inequivalent n.n bonds [10].  $\mathbf{H}$  is the external field in the corresponding energy units.

Here and below we use tildes over symbols for Fe-related parameters.

It is known experimentally that the Fe moments lie within the  $ab$  plane and are oriented along the longer  $a$  axis (i.e.,  $\tilde{D} > 0$ ). Neutron scattering provides estimates for the parameters as  $\tilde{J} \sim 30$  meV,  $\tilde{D} \approx 0.25$  meV [11]. Minimizing Eq. (1) with respect to  $\mathbf{f}$ , for  $\mathbf{H}\parallel b$  (no linear susceptibility appears for  $\mathbf{H}\parallel a$ ), we observe that  $H$  generates a canting of the Fe spins away from the  $a$  axis by an angle  $\tilde{\alpha} = \sin^{-1}(\tilde{M}H/4\tilde{J})$ , which corresponds to an energy gain of  $E = (\tilde{M}H)^2/4\tilde{J}$  per formula unit (f.u). There are two ways the system may take advantage of this energy gain, even if the field is along  $a$ . First, all Fe spins may rearrange (abruptly) from being aligned along  $a$  to being predominantly aligned along  $b$ . This process is called spin-flop and occurs when  $\tilde{J} > \tilde{D}$ . Using  $\tilde{M} \approx 1\mu_{\text{B}}$  and the above parameters, we estimate  $\tilde{H}^{\text{flop}} = 2\sqrt{2\tilde{D}\tilde{J}}/\tilde{M} \approx 11$  meV  $\approx 135$  T. Thus, the spin-flop never occurs at typically lab-accessible fields. The other way is to switch an entire ‘‘a-twin’’ (i.e., a domain with antiferromagnetic bonds along the crystallographic  $a$  in the field direction) to a b-twin (in other words, to rotate the crystal structure by  $90^\circ$  around  $c$ , keeping the moments aligned along the

magnetic easy  $a$  axis. This process is associated with an unknown energy barrier  $\Delta$ . Given that in the field of approximately 15 T, the Stanford group has observed partial [6] and, in approximately 30 T, nearly full detwinning [7], we deduce  $\Delta \sim E = (\tilde{M}H)^2/4\tilde{J} \approx 0.025$  meV/f.u.

One can verify these deductions against mechanical detwinning. The latter is an indirect process wherein it is difficult to access the microscopic strain and stress. Reported values for the latter differ from  $\sigma = 6\text{--}20$  MPa [12,13]. Assuming  $\sigma = 10$  MPa and taking the elastic modulus to be 10 GPa [14,15], we derive a strain of  $\varepsilon \approx 0.1\%$ . Finally, using the calculated dependence of the total energy on the microscopic strain [16], we find that this strain corresponds to  $\Delta \approx 0.01$  meV/f.u., which is in agreement with our magnetic estimate.

Yet another estimate can be obtained by considering the stress  $\sigma$  on the unit cell during mechanical detwinning and calculate the energy associated with the displacement  $\delta$  from  $a\parallel\sigma$  to  $b\parallel\sigma$ . Using the reported lattice parameters of  $\text{EuFe}_2\text{As}_2$  [17], we arrive at  $\delta = 1.6 \times 10^{-12}$  m. Assuming  $\sigma = 6$  MPa, this leads also to an energy of  $\Delta \approx 0.01$  meV/f.u.

Given that the detwinning energy, according to this theory, depends quadratically on the magnetic moment, and inversely on the exchange constant, one may naively assume that the same mechanism will be operative in  $\text{EuFe}_2\text{As}_2$ , given that the ordering temperature in the Eu sublattice is much smaller,  $T_N = 19$  K, and the moment much larger,  $M = 7\mu_B$ , than for the Fe sublattice. Such a phenomenology was adapted in Ref. [9] in order to parametrize the observed effect. However, it is easy to see that it is microscopically untenable. Indeed, while it is possible and reasonable to write down interactions *inside* the Eu sublattice in Heisenberg form,

$$\mathcal{H}_{\text{Eu}} = J_{\parallel} \sum_{\langle ij \rangle} \mathbf{e}_i \cdot \mathbf{e}_j + J_{\perp} \sum_i \mathbf{e}_i \cdot \mathbf{e}_{i^+} - M \sum_i \mathbf{e}_i \cdot \mathbf{H}, \quad (2)$$

where  $i, j$  label Eu sites;  $i^+$  the opposing Eu site in the next layer;  $\mathbf{e}_i$  the unit vectors directed along the Eu magnetic moment  $M$  at site  $i$ ; and the ferromagnetic  $J_{\parallel} < 0$  and antiferromagnetic  $J_{\perp} > 0$  constants determine the in-plane and interplanar ordering, respectively, it is not possible to describe the interaction between the Fe and Eu subsystems in the same manner, for the simple reason that the Heisenberg exchange field induced by the Fe planes on the Eu sites is zero by symmetry. In fact, any bilinear coupling between the Fe stripes and in-plane Eu spins is zero by symmetry, including Heisenberg, Dzyaloshinsky-Moria, and dipole interaction (in the last case, the field induced by the Fe planes on the Eu sites is nonzero, but it is directed strictly along  $z$ ; see Supplemental Material [18]). Note that we did not include any single-site anisotropy in Eq. (2), because Eu adopts a valence state of  $+2$  in this system. Due to the closed  $f$  shell, with seven electrons in the spin-majority channel,  $\text{Eu}^{2+}$  has zero angular

momentum and negligible magnetocrystalline anisotropy. This is confirmed by first-principles calculations, presented in the Supplemental Material [18] to this article. Without an interaction between Fe and Eu, there is no physical mechanism by which the Eu spin dynamics may affect the detwinning.

Another intriguing problem, possibly related to this one, is the fact that even the basic magnetic properties of  $\text{EuFe}_2\text{As}_2$  cannot be explained within a simple Heisenberg model. Indeed, the magnetic susceptibility of  $\text{EuFe}_2\text{As}_2$  above  $T_N$  is dominated by the Eu spins and well described by a nearly isotropic Curie-Weiss law, in accordance with the previous paragraph. Equation (2) suggests that  $k_B T_{\text{CW}} = \frac{3}{7}(4J_{\parallel} - 2J_{\perp})$  [the quantum prefactor  $3M/(M+2)$  would have been 1 if  $M$  were  $1\mu_B$ , but for  $M = 7\mu_B$ , it becomes  $3/7$ ]. The effective moment has been determined to be  $M = 7\mu_B$ , with  $T_{\text{CW}} \approx -20$  K [19]. Thus the Néel temperature appears to be equal to the mean-field transition temperature of the individual Eu planes. In other words, each Eu plane orders magnetically at the mean-field temperature, not at all suppressed by fluctuations, and immediately at the transition, the antiferromagnetic stacking of the individual planes along  $c$  is acquired.

At this point, it is instructive to look at first-principles calculations and what they tell us about  $J_{\perp}$  and  $J_{\parallel}$ . The former appears to be very small and decreases with the value of the Hubbard  $U$  used on the Eu  $f$  orbitals. This is not surprising, because it is set by the competition between superexchange, proportional to  $t_{\perp}^2/U$ , and Schrieffer-Wolff-driven [20] double exchange, proportional to  $(t_{\text{Eu-Fe}}^2/U)^2 N(0)$ , with  $N(0)$  the density of states, and  $t_{\perp}$  and  $t_{\text{Eu-Fe}}$  the effective Eu-Eu and Eu-Fe hopping across the planes. For  $U - J = 0$ , we get  $J_{\perp} = 0.14$  meV (1.6 K) and  $J_{\parallel} = -2$  meV (23 K), while for  $U - J = 5$  eV, we find  $J_{\perp} = 0.26$  meV (3 K) and  $J_{\parallel} = -0.8$  meV (9 K). The LDA +  $U$  results, which we believe are closer to reality, correspond to  $T_{\text{CW}} \sim -13$  K, and  $T_N \approx 4.27J_{\parallel}/[3.12 + \log(J_{\parallel}/J_{\perp})] = 9$  K for the Heisenberg model [21]. The ratio  $T_{\text{CW}}/T_N$  is close to 1.4 rather than the experimental 1.13, and one can see that in order to reduce it to 1.13, one needs to increase the  $J_{\perp}/J_{\parallel}$  ratio to approximately 0.5, a rather unrealistic three-dimensionality.

The situation could be remedied if one were to assume a finite single-site anisotropy for Eu of  $D \approx 1$  K, because in such a case, one has to replace  $J_{\perp}$  with  $J_{\text{eff}} = J_{\perp} + D + \sqrt{D^2 + 2J_{\perp}D}$  [22,23], which leads to a sufficient increase of the Néel temperature and consequently to  $T_{\text{CW}}/T_N = 1.13$ . But, as we have argued above,  $\text{Eu}^{2+}$  has no single-site anisotropy. One of the results of our paper, however, is that a biquadratic coupling  $K$  between the Eu and Fe subsystems is operative in  $\text{EuFe}_2\text{As}_2$ , which plays the key role in its magnetic detwinning. This interaction acts as an *effective anisotropy* for the Eu

subsystem, which tries to imprint the orientation of the Fe spins on the Eu spins. The corresponding number ( $8K$ ) that we extract from the experiment amounts to  $D_{\text{eff}} \sim 0.6$  K. Substituting this into the formulas above, we get  $T_{\text{CW}}/T_{\text{N}} \approx 1.18$ , which is within the error margin of the experimental ratio. Of course, given the model character of these calculations, a discrepancy of approximately 25% is not too alarming. However, it is noteworthy that after adding the experimentally determined biquadratic term, the discrepancy virtually disappears completely.

Note that, unlike correlated insulators, FeBS have a considerable biquadratic interaction within the Fe subsystem, which plays a crucial role in their nematic behavior [24]. Whether this is a universal property of correlated magnetic metals, which simply had not been given proper attention before, or is unique for FeBS is unknown. With this in mind, we have combined the Hamiltonians from Eqs. (1) and (2) in the following way:

$$\begin{aligned} \mathcal{H} = & -\tilde{M} \sum_{\alpha} \mathbf{f}_{\alpha} \cdot \mathbf{H} + \tilde{J} \sum_{\langle \alpha\beta \rangle} \mathbf{f}_{\alpha} \cdot \mathbf{f}_{\beta} - \tilde{D} \sum_{\alpha} f_{\alpha a}^2 \\ & - M \sum_i \mathbf{e}_i \cdot \mathbf{H} + J_{\perp} \sum_i \mathbf{e}_i \cdot \mathbf{e}_{i^+} \\ & - K \sum_{\alpha, n} (\mathbf{f}_{\alpha} \cdot \mathbf{e}_{\alpha+n})^2, \end{aligned} \quad (3)$$

where the greek subscripts label the Fe sites, Latin the Eu sites, and the last summation runs over all n.n Fe-Eu pairs. We have then estimated the biquadratic Eu-Fe coupling

$$\begin{aligned} \mathcal{E} = & -\tilde{M}H(\cos \tilde{\varphi}_1 + \cos \tilde{\varphi}_2) + 2\tilde{J} \cos(\tilde{\varphi}_2 + \tilde{\varphi}_1) - \tilde{D}(\cos^2 \tilde{\alpha}_1 + \cos^2 \tilde{\alpha}_2) \\ & - MH(\cos \varphi_1 + \cos \varphi_2)/2 + J_{\perp} \cos(\varphi_2 + \varphi_1) \\ & - 2K[\cos^2(\varphi_2 - \tilde{\varphi}_2) + \cos^2(\varphi_2 - \tilde{\varphi}_1) + \cos^2(\varphi_1 - \tilde{\varphi}_2) + \cos^2(\varphi_1 - \tilde{\varphi}_1)], \end{aligned} \quad (4)$$

where  $\alpha$ 's are the Fe angles measured from the magnetic easy  $a$  axis.

For the b-twin domains and low fields, i.e.,  $\tilde{\varphi}_2 = \tilde{\varphi}_1 = \pi/2$ ,  $\varphi_1 = \varphi_2 = \varphi$ ,  $\tilde{\alpha}_2 = \tilde{\alpha}_1 = 0$ , this yields

$$E_b = -MHp(2J_{\perp} + 8K)p^2 + E_0, \quad (5)$$

where we have expressed everything in terms of  $p = \cos \varphi$  and  $E_0 = -2\tilde{J} - 2\tilde{D} - J_{\perp} - 8K$ . The equilibrium tilting angle and energy are given by

$$p_b^{\min} = \frac{MH}{4J_{\perp} + 16K} \quad (6)$$

$$E_b^{\min} = -\frac{(MH)^2}{8(J_{\perp} + 4K)} + E_0. \quad (7)$$

term  $K$  from LDA + U calculations (see Supplementary Material [18]) and obtained an estimate of  $K \sim 0.4$  meV. Given the uncertainty in the calculations, this should be taken as evidence that  $K$  is not negligible; later, we will determine the actual amplitude of  $K$  directly from the experiment.

In the Supplemental Material [18], we present detailed derivations of the solutions of Eq. (3) for both possible orientations of the external field with respect to the crystallographic axes and for all relevant field regimes. The discussion below omits less relevant parts of the full theory, concentrating on rationalizing the actual experimental observations.

### III. DOMAIN ENERGETICS

We start our discussion in the *low-field* regime, that is,  $0 < H \lesssim H_1 \sim 1$  T, before considering higher fields. In this regime, the Fe single-site anisotropy dominates, and Fe spins are always oriented along the crystallographic  $a$  axis. So are, initially, Eu spins. We will distinguish two cases: first, when  $\mathbf{H}$  is applied perpendicular to the initial orientation of Eu spins (b-twin) or, second, parallel to them (a-twin). In this regime, the former is always lower in energy, since the latter has formally zero spin susceptibility. We will characterize the orientation of the Eu and Fe spins by their respective angles  $\varphi$  and  $\tilde{\varphi}$  with respect to the external field. Figure 1(a) is drawn for a b-twin domain, i.e.,  $a \perp H$ . Equation (3) can then be rewritten in terms of these angles (per one formula unit) as

The biquadratic term in the definition of  $E_0$  is always trying to minimize the angle between the Fe spins and Eu spins. Thus, in simplified terms (see Supplementary Material [18] for details), if  $\pi/4 < \varphi < \pi/2$ , Fe spins prefer to orient perpendicular to the field ( $\tilde{\varphi} = \pi/2$ ), and the b-twin domain is always lower in energy. When  $\varphi$  becomes smaller than  $\pi/4$ , it becomes more favorable to orient Fe spins parallel to the field ( $\tilde{\varphi} = 0$ ), and this is the first critical field  $H_1$  at which the first domain reorientation from b-twins to a-twins takes place (note that in this field regime, only  $\tilde{\varphi} = \pi/2$ , or, in the case of the a-twin, 0, is allowed; any intermediate value of  $\tilde{\varphi}$  is severely punished by the Fe-Fe exchange and single-site anisotropy).

After this reorientation has occurred, the total energy is expressed as

$$E_a = -MHp + (2J_{\perp} - 8K)p^2 + E_0 + 8K, \quad (8)$$

and consequently,

$$p_a^{\min} = \frac{MH}{4J_{\perp} - 16K} \quad (9)$$

$$E_a^{\min} = -\frac{(MH)^2}{8(J_{\perp} - 4K)} + E_0 + 8K. \quad (10)$$

Thus, the first reorientation field  $H_1$  is defined by  $E_a^{\min} = E_b^{\min}$ , or

$$H_1 = \frac{2}{M} \sqrt{2(J_{\perp}^2 - 16K^2)}. \quad (11)$$

At the field  $H_a^{\text{sat}} = 4(J_{\perp} - 4K)/M$ , the angle  $\varphi$  becomes 0; that is to say, Eu spins are perfectly aligned with the field. Further increase of the field does not change the total energy (aside from the Zeeman term  $-MH$ ), because from that point on the differential spin susceptibility of the Eu subsystem becomes zero. However, while theoretically important, this field does not manifest itself as a change of regime in domain dynamics.

$H_a^{\text{sat}}$  is too small to incur any Fe spin dynamics, but, in principle, with further increase of  $H$  one needs to include the spin susceptibility of the Fe subsystem. The latter is zero as long as Fe spins are parallel to Eu spins, satisfying the biquadratic coupling. Yet, in a sufficiently strong field, i.e., at  $H \gtrsim H_2$ , a potential energy gain from allowing Fe spins to screen the field outweighs the loss of the biquadratic interaction. Mathematically, the latter, in this regime  $H > H_a^{\text{sat}}$ , is reduced to an effective single-site anisotropy for the Fe subsystem, subtracting from the actual anisotropy, and the transition in question is described by the same formulas as a typical spin-flop transition. We can find the corresponding field value in the same way as one derives the spin-flop field in textbooks: we need the energy gain from the Fe spin-flop to overcome the energy loss due to noncollinearity (the loss occurs both because of the Fe-Fe exchange  $\tilde{J}$  and because the Fe site anisotropy is much larger than the biquadratic coupling).

In this case, the total energy (since now  $\varphi = 0$ ,  $\tilde{\alpha} = \pi/2 - \tilde{\varphi}$ ) is

$$\begin{aligned} \tilde{E}_b = & -2\tilde{M}H\tilde{p} + 2(2\tilde{J} + \tilde{D} - 4K)\tilde{p}^2 \\ & - MH + E_0 + 2J_{\perp} + 8K, \end{aligned}$$

where we have now used  $\tilde{p} = \cos \tilde{\varphi}$  and  $E_0$ . Minimizing with respect to  $\tilde{p}$  yields

$$\tilde{p}_b^{\min} = \frac{\tilde{M}H}{2(2\tilde{J} + \tilde{D} - 4K)},$$

with the energy gain compared to Eq. (8), with  $p = 1$ , being

$$dE = +\frac{(\tilde{M}H)^2}{2(2\tilde{J} + \tilde{D} - 4K)} - 8K.$$

This expression changes sign at  $H_2 = 4\sqrt{2\tilde{J}K + \tilde{D}K - 4K^2} / \tilde{M} \approx 4\sqrt{2\tilde{J}K} / \tilde{M}$ . This is the second critical field at which the reorientation back to the b-twin domains is initiated.

The domain dynamics, with the initial detwinning to b-twins at  $H_0$ , first reorientation to a-twins at  $H_1$ , and second reorientation back to b-twins at  $H_2$ , is illustrated in Figs. 1(b)–1(h) and also in a supplemental movie ([18]). There, we depict how Eu and Fe spins (and the structural axes follow the latter) rotate in an external field. One can see that, despite the physical simplicity, the actual dynamics is rather complicated.

#### IV. DETERMINATION OF THE COUPLING CONSTANTS

While the  $H_{0,1,2}$  defined above directly manifest themselves in the experiment, the actual expression for the energy difference between the two types of domains (which is needed to describe domain dynamics, as opposed to the thermodynamic equilibrium) is a complicated piecewise function of the field. The full derivation can be found in the Supplemental Material [18], where explicit expressions for all critical fields are obtained. In the relevant field range for the experiments discussed here, this function is given by

$$dE = \begin{cases} \frac{M^2 H^2}{8(J_{\perp} + 4K)}, & \{0, H_a^{\text{flop}}\} \\ K \left( 8 - \frac{M^2 H^2}{J_{\perp}^2 - 16K^2} \right), & \{H_a^{\text{flop}}, H_a^{\text{sat}}\} \\ -MH + 2J_{\perp} + \frac{M^2 H^2}{8(J_{\perp} + 4K)}, & \{H_a^{\text{sat}}, H_b^{\text{sat}}\} \\ -8K + \frac{\tilde{M}^2 H^2}{2(2\tilde{J} + \tilde{D} - 4K)}, & \{H_b^{\text{sat}}, H_2\}. \end{cases} \quad (12)$$

In the second case,  $dE > 0$  changes to  $dE < 0$  at  $H_1$ , which lies between  $H_a^{\text{flop}}$  and  $H_a^{\text{sat}}$ . The fields  $H_1$ ,  $H_a^{\text{sat}}$ , and  $H_2$  have been derived above. The transformations associated with  $H_a^{\text{flop}}$  and  $H_b^{\text{sat}}$  occur in “wrong,” or minority domains, which are thermodynamically unstable, but occur kinetically. Their expressions, as derived in the Supplemental Material [18], are  $H_b^{\text{sat}} = 4(J_{\perp} + 4K)/M$  and  $H_a^{\text{flop}} = 8/M\sqrt{K(J_{\perp} - 4K)}$ .

The coupling constants  $J_{\perp}$  and  $K$  can be determined from experiment. Magnetization, magnetostriction, neutron, and magnetotransport measurements, for instance, all can be used to estimate the domain population ratio. In the following, we will determine the coupling constants using new magnetization data [9] and then use them to calculate

this ratio as a function of field in order to compare it to the experiment.

When measured along the tetragonal  $[110]_T$  direction, a roughly linear magnetization  $M(H)$  was reported in Ref. [9], interrupted only by two pronounced jumps around 0.1 T and 0.6 T. Saturation sets in above 0.9 T with  $M \approx 5\mu_B$ . Due to the uncharacteristically small saturated moment, which does not agree well with previously published data [19], and the theoretically expected value of  $M = 7\mu_B$ , we have remeasured the magnetization of a  $\text{EuFe}_2\text{As}_2$  sample from Zapf *et al.* [9]. The results are shown in Fig. 2 for decreasing magnetic field. The overall behavior is similar, but we found a saturation magnetization of  $6.82\mu_B$ , in good agreement with the theoretical expectations and Ref. [19].

The steplike increase of the magnetization around  $0.65\mu_B\text{T}$  was associated with a spin-flip transition of the  $\text{Eu}^{2+}$  moments in Ref. [9]. However, magnetostriction, magnetotransport, and unpublished neutron diffraction data indicate that the feature is associated with the reorientation of domains, rather than an intrinsic spin-flip of the a-twin domain and must, therefore, be identified with  $H_1$ . Furthermore, the Eu saturation field of the b-twin domain can be extrapolated to  $H_b^{\text{sat}} \approx 1.14$  T from the slope of the low-field region between 0.2 T and 0.5 T (Fig. 2); note that this field needs to be extrapolated, and it cannot be measured directly because at  $H \gtrsim 1$  T virtually all domains are a-twins [Fig. 1(g)]. The constants can be extracted from these two fields using the following set of equations:

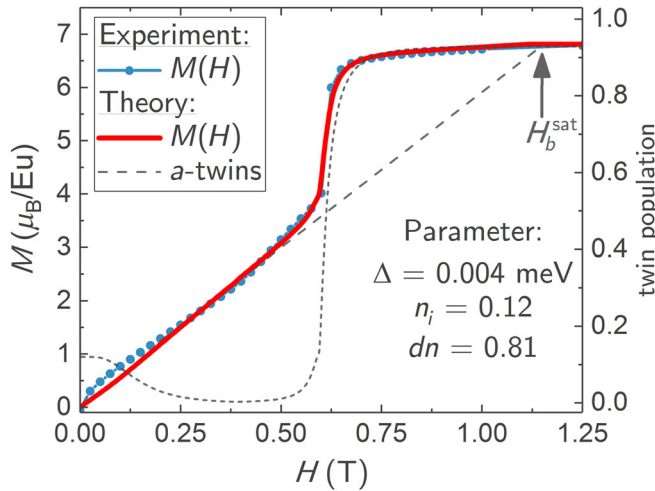


FIG. 2. Magnetization at ( $T = 5$  K) as a function of decreasing magnetic field applied along the  $[110]_T$  direction (blue symbols) remeasured from Zapf *et al.* [9]. The solid line (red) represents our theoretical prediction using the determined coupling constants. The short dashed line depicts the a-twin domain population  $n$  derived from a fit to the corresponding magnetoresistance data, similar to Fig. 5, yielding  $\Delta = 0.004$  meV,  $n_i = 0.12$ , and  $dn = 0.81$  (see Supplemental Material [18]). The long dashed line depicts the extrapolation of  $H_b^{\text{sat}}$ , as discussed in the text.

$$\begin{aligned} J_{\perp} &= \frac{M}{8} H_b^{\text{sat}} \left[ 1 + 2 \left( \frac{H_1}{H_b^{\text{sat}}} \right)^2 \right] \\ K &= \frac{M}{32} H_b^{\text{sat}} \left[ 1 - 2 \left( \frac{H_1}{H_b^{\text{sat}}} \right)^2 \right], \end{aligned} \quad (13)$$

which yields  $J_{\perp} = 0.093(11)$  meV and  $K = 0.0049(18)$  meV for this particular sample.

The determination of the coupling constants via a different set of equations is discussed in the Supplemental Material [18]. The respective results are summarized there in Table SII. We have cross-checked the results by determining the parameters from various samples grown with different methods and investigated with various measurements techniques like magnetostriction, magnetotransport, and neutron diffraction data. The results appear to be consistent between measurements, but we found a noticeable sample dependence, which also seems to be related to the synthesis methods of the single crystals; see also Table SII. The averaged values are  $J_{\perp} = 0.121(24)$  meV,  $K = 0.0072(22)$  meV, and  $J_{\perp}/K \approx 18(4)$ . However, since each Eu atom is surrounded by 8 Fe atoms,  $8K = 0.057$  meV is the more representative quantity to gauge the biquadratic coupling strength in the system.

## V. ENERGY BARRIER AND DOMAIN DYNAMICS

The domain dynamics are driven by the energy difference  $dE$  between the domains. In Fig. 3, we show  $dE$  on

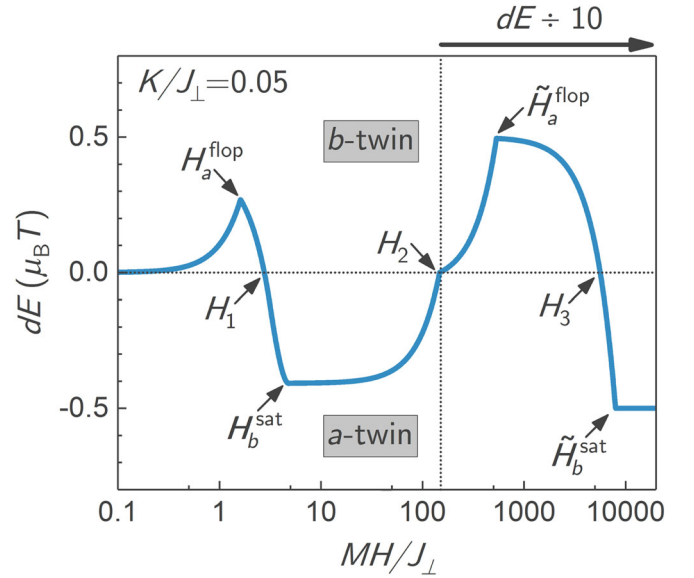


FIG. 3. Calculated domain energy difference  $dE$  as a function of  $MH/J_{\perp}$  for a characteristic ratio of  $K/J_{\perp} = 0.05$ . For better visibility, values above  $H_2$  (vertical dashed line) are rescaled by a factor of 10. Positive values and negative values correspond to the b-twin and a-twin domain, respectively. The horizontal dashed line indicates  $dE = 0$ .

a semilog plot as a function of the reduced variable  $MH/J_{\perp}$  for a representative ratio of  $K/J_{\perp} = 0.05$ . Positive values correspond to the b-twin domain being the ground state, while for negative ones, the a-twin is the ground state. The phase diagram in thermodynamic equilibrium over a large parameter space in reduced coordinates  $\{K/J_{\perp}, MH/J_{\perp}\}$  is shown in Fig. 4. The remainder of the formulas used in constructing this phase diagram can be found in the Supplemental Material [18].

Until now, we have assumed that the reorientation of twin domains has no energy cost. In reality, however, there is an unknown energy barrier  $\Delta$  associated with the reorientation; i.e., the energy difference  $dE = E_{a\text{-twin}} - E_{b\text{-twin}}$  between the two twin variants needs to exceed a certain threshold before reorientation occurs. In the following, we will assume  $\Delta$  for various domain walls to be log-normal distributed; i.e.,  $\log \Delta$  is normal [25]. This is a typical distribution, e.g., of grain sizes in polycrystalline matter [26]. The cumulative distribution function  $F_X(x)$  of a positive log-normal distributed variable  $X$  is given by  $F_X(x) = \frac{1}{2} \operatorname{erfc}\left\{-\frac{(\log x - \mu)}{\sigma\sqrt{2}}\right\}$ , with the location and the scaling parameters  $\mu$  and  $\sigma$ . Because  $dE$  changes sign as a function of applied field, the log-normal distribution in our case leads to the following fit function to the (a-twin) domain population:

$$n(dE) = \begin{cases} n_0 \cdot \frac{1}{2} \operatorname{erfc}\left(\frac{\log(dE/\Delta)}{\sqrt{2}}\right), & dE > 0 \\ dn \cdot \frac{1}{2} \operatorname{erfc}\left(-\frac{\log(-dE/\Delta)}{\sqrt{2}}\right) + n_0, & dE < 0 \end{cases},$$

with  $n_0$  the fraction of a-twins at  $H = 0$  and  $dn = n_{\text{sat}} - n_0$  the difference between the saturated a-twins  $n_{\text{sat}}$  and  $n_0$ . Together with Eq. (12), this function fully describes the domains' population.

Prior to performing the fit, the domain population needs to be extracted from the available measurements. The domain population  $n(H)$  can be determined in a variety of ways. Arguably the most exact data can be extracted from field-dependent neutron diffraction measurements on a free-standing sample, which will be published soon [27]. In the following, we will use magnetostriction (MS) data by Zapf *et al.* [9], which agree with the preliminary data of Ref. [27].

The MS is defined as  $\Delta L(H)/L_0 = (L(H) - L_0)/L_0$ , where  $L_0$  and  $L(H)$  are the initial and field-dependent average unit cell length, respectively. They can be expressed by  $L(H) = n(H)a + [1 - n(H)]b$  and  $L_0 = n_0a + (1 - n_0)b$ , again with the (initial) domain population  $n_0$  at  $H = 0$  and orthorhombic lattice parameters  $a$  and  $b$ . Solving for  $n$  leads to

$$n(H) = \frac{\Delta L}{L_0} \left( \frac{b}{a - b} + n_0 \right),$$

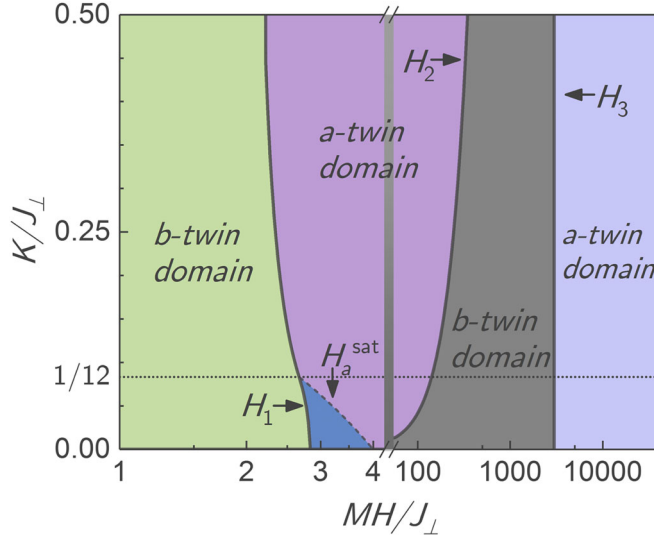


FIG. 4. Phase diagram  $K/J_{\perp}$  vs  $MH/J_{\perp}$  in thermodynamic equilibrium. The four phases shown correspond to the b-twin domains (green) with canted  $\text{Eu}^{2+}$  spins, a-twin domains with saturated (purple) or unsaturated (blue) Eu magnetization, respectively, followed by the b-twin domains (gray) induced by the canting of Fe spins. Finally, another hypothetical phase of a-twin domains, induced by further canting of the Fe spins, is shown (light blue). More details, also on the significance of the dotted line, indicating  $12K/J_{\perp} = 1$ , can be found in the Supplemental Material [18].

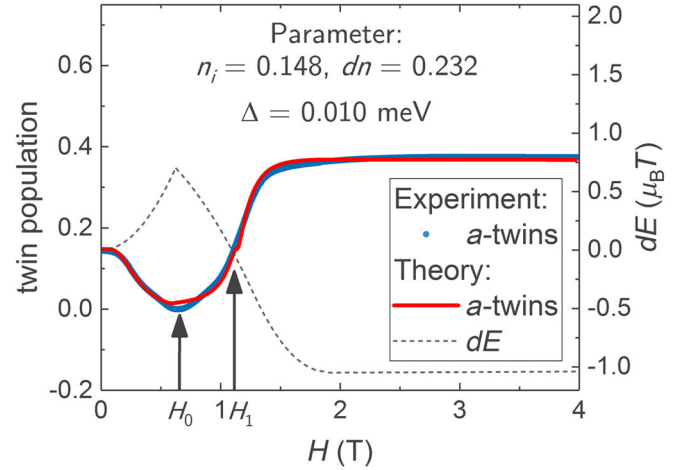


FIG. 5. Twin domain population derived from magnetostriction data at  $(T = 5 \text{ K})$  from Ref. [9] as a function of (increasing) magnetic field applied along the  $[110]_{\text{T}}$  direction (blue line) as discussed in the main text. The solid line (red) represents the theoretical prediction using the constants' values derived in the main text and the Supplemental Material [18] (see Table SII, #2). The dashed line (gray) depicts the theoretically derived domain energy difference  $dE$ , similar to Fig. 3(b). The a-twin domain population is reduced, because of the pressure of the dilatometer, which favors the b-twin domain in this orientation.

from which follows

$$n_0 = \frac{a \cdot n(H) - b[n(H) + \Delta L/L_0]}{(a - b)(1 + \Delta L/L_0)}, \quad (14)$$

assuming full detwinning at the observed minimum around  $H_0$ , with  $b \parallel H$ , i.e.,  $n(H_0) = 0$ . This assumption is justified, as preliminary neutron data [27] indicate a domain distribution with  $n(H_0) = 0.06$ . Furthermore, the significant pressure of the dilatometer in field direction, 1.35 MPa [9], aids the  $n = 0$  alignment at small magnetic fields (but hinders it at larger fields, when  $n \rightarrow 1$ ). The extracted domain population is shown in Fig. 5. The solid red line represents the fit to the data (blue symbols). The energy barrier for this particular sample and measurement technique was determined to be  $\Delta = 0.01$  meV. Among the other investigated samples,  $\Delta$  ranges roughly between  $10^{-3}$  meV and  $10^{-2}$  meV, in agreement with the estimates presented in the Introduction.

## VI. CONSISTENCY CHECK

Using the averaged constants from the previous paragraph, we find  $H_1 = 0.85$  T and  $H_2 = 35$  T, in very good agreement with experiment. Utilizing the knowledge about the energy barrier, we can also calculate the initial detwinning field from the condition  $dE = \Delta$ , through

$$H_0 = \frac{2}{M} \sqrt{2\Delta(J_{\perp} + 4K)}.$$

For the determined  $\Delta$  range between 0.001 meV and 0.01 meV, this yields 0.09 T to 0.28 T, which is also in excellent agreement with the experimental evidence.

Going even further, the presented theory allows us to calculate our new magnetization data, by weighting the Eu magnetization of the twin sublattices with the domain population  $n(H)$  (dashed line in Fig. 2), which we calculated using  $\Delta = 0.004$  meV,  $n_i = 0.22$ , and  $dn = 0.71$ . The total magnetization is given by

$$M(H) = n(H) \cdot M_a + (1 - n(H)) \cdot M_b, \quad (15)$$

where  $M_a$  and  $M_b$  are the magnetization of the sublattices given by  $M \cos \varphi$ , i.e.,

$$M_a = \begin{cases} 0, & \{0, H_a^{\text{flop}}\} \\ \frac{M^2 H}{4(J_{\perp} - 4K)}, & \{H_a^{\text{flop}}, H_a^{\text{sat}}\} \\ M, & \{H_a^{\text{sat}}, \infty\}, \end{cases}$$

$$M_b = \begin{cases} \frac{M^2 H}{4(J_{\perp} + 4K)}, & \{0, H_b^{\text{sat}}\} \\ M, & \{H_b^{\text{sat}}, \infty\}. \end{cases}$$

The result is depicted by the solid red line in Fig. 2.

## VII. SUMMARY

We present a microscopic, physically meaningful and quantitative description of the observed magnetic detwinning effect in FeBS, with all its complexity. In particular, the following mysteries have been resolved: (i) strong detwinning in minuscule fields despite the absence of spin-orbit coupling effects in  $\text{Eu}^{2+}$  ions; (ii) coupling of Eu spin orientation to the Fe sublattice, despite any bilinear interaction canceling out by symmetry; and (iii) double reversal of the preferential domain orientation with the increase of the external field. We show that all these issues find a natural explanation if a *biquadratic* Eu-Fe coupling is included in the model. We also show that such a term does actually appear in first-principles calculation, with an amplitude even stronger than needed to explain the experimental data. Furthermore, we were able to describe quantitatively not only the thermodynamic phase diagram, but even the dynamics of detwinning (as deduced from our new magnetization data), assuming that the detwinning energy barriers are distributed according the log-normal law (quite typical in crystal morphology).

Although we focus on the Eu-based 122 system, our findings should be of great interest for other large-spin rare earths as well, such as the Gd-based 1111 compound, which, like  $\text{EuFe}_2\text{As}_2$ , also features large  $S = 7/2$  spin-only moments, or the recently discovered Eu-based 1144 systems. Furthermore, the theory also captures the physics of the high-field ( $H \gtrsim 15$  T) detwinning, which occurs even in non-Eu-based iron pnictides. The microscopic understanding of the phenomenon of magnetic detwinning in ultralow magnetic fields, as deduced above, opens new avenues for the experimental investigation of spin-driven nematicity in Fe-based superconductors.

## ACKNOWLEDGMENTS

We are grateful to Shibabrata Nandi and Yinguo Xiao for giving us access to their neutron diffraction data, to Makariy Tanatar for sharing with us his data on mechanical detwinning, and to Ian Fisher for discussing with us the concept of this work. We would also like to convey our gratitude to Shuai Jiang, Christian Stingl, and H. S. Jeevan for permitting us access to their samples and magnetostriction data; to Sina Zapf and Martin Dressel for collaboration in the early stage of this project (Ref. [9]); and to James Glasbrenner for verifying our biquadratic calculations using an all-electron method. J. M. thanks Patrick Seiler for support and discussions. J. M. and P. G. are supported by DFG through SPP 1458. I. I. M. is supported by ONR through the NRL basic research program.

[1] I. R. Fisher, L. Degiorgi, and Z. X. Shen, *In-Plane Electronic Anisotropy of Underdoped “122” Fe-Arsenide*

- Superconductors Revealed by Measurements of Detwinned Single Crystals*, *Rep. Prog. Phys.* **74**, 124506 (2011).
- [2] M. A. Tanatar, A. Kreyssig, S. Nandi, N. Ni, S. L. Bud'ko, P. C. Canfield, A. I. Goldman, and R. Prozorov, *Direct Imaging of the Structural Domains in the Iron Pnictides*  $\text{AFe}_2\text{As}_2$  ( $A = \text{Ca, Sr, Ba}$ ), *Phys. Rev. B* **79**, 180508 (2009).
- [3] A. N. Yaresko, G.-Q. Liu, V. N. Antonov, and O. K. Andersen, *Interplay between Magnetic Properties and Fermi Surface Nesting in Iron Pnictides*, *Phys. Rev. B* **79**, 144421 (2009).
- [4] A. L. Wysocki, K. D. Belashchenko, and V. P. Antropov, *Consistent Model of Magnetism in Ferropnictides*, *Nat. Phys.* **7**, 485 (2011).
- [5] G. Zhang, J. K. Glasbrenner, R. Flint, I. I. Mazin, and R. M. Fernandes, *Double-Stage Nematic Bond Ordering above Double Stripe Magnetism: Application to  $\text{BaTi}_2\text{Sb}_2\text{O}$* , *Phys. Rev. B* **95**, 174402 (2017).
- [6] J.-H. Chu, J. G. Analytis, D. Press, K. De Greve, T. D. Ladd, Y. Yamamoto, and I. R. Fisher, *In-Plane Electronic Anisotropy in Underdoped  $\text{Ba}(\text{Fe}_{1-x}\text{Co}_x)_2\text{As}_2$  Revealed by Partial Detwinning in a Magnetic Field*, *Phys. Rev. B* **81**, 214502 (2010).
- [7] J. P. C. Ruff, J.-H. Chu, H.-H. Kuo, R. K. Das, H. Nojiri, I. R. Fisher, and Z. Islam, *Susceptibility Anisotropy in an Iron Arsenide Superconductor Revealed by X-Ray Diffraction in Pulsed Magnetic Fields*, *Phys. Rev. Lett.* **109**, 027004 (2012).
- [8] Y. Xiao, Y. Su, W. Schmidt, K. Schmalzl, C. M. N. Kumar, S. Price, T. Chatterji, R. Mittal, L. J. Chang, S. Nandi, N. Kumar, S. K. Dhar, A. Thamizhavel, and Th. Brueckel, *Field-Induced Spin Reorientation and Giant Spin-Lattice Coupling in  $\text{EuFe}_2\text{As}_2$* , *Phys. Rev. B* **81**, 220406(R) (2010).
- [9] S. Zapf, C. Stingl, K. W. Post, J. Maiwald, N. Bach, I. Pietsch, D. Neubauer, A. Löhle, C. Clauss, S. Jiang, H. S. Jeevan, D. N. Basov, P. Gegenwart, and M. Dressel, *Persistent Detwinning of Iron-Pnictide  $\text{EuFe}_2\text{As}_2$  Crystals by Small External Magnetic Fields*, *Phys. Rev. Lett.* **113**, 227001 (2014).
- [10] It is well established that a microscopically justifiable model includes Heisenberg terms up to the third neighbors and a sizable n.n biquadratic coupling [4], but for our purpose of calculating the spin canting in an external magnetic field and the corresponding energy gain, all this complexity can be absorbed in one parameter, of which we only need to know the order of magnitude.
- [11] C. Wang, R. Zhang, F. Wang, H. Luo, L. P. Regnault, P. Dai, and Y. Li, *Longitudinal Spin Excitations and Magnetic Anisotropy in Antiferromagnetically Ordered  $\text{BaFe}_2\text{As}_2$* , *Phys. Rev. X* **3**, 041036 (2013).
- [12] S. Jiang, H. S. Jeevan, J. Dong, and P. Gegenwart, *Thermopower as a Sensitive Probe of Electronic Nematicity in Iron Pnictides*, *Phys. Rev. Lett.* **110**, 067001 (2013).
- [13] E. C. Blomberg, A. Kreyssig, M. A. Tanatar, R. M. Fernandes, M. G. Kim, A. Thaler, J. Schmalian, S. L. Bud'ko, P. C. Canfield, A. I. Goldman, and R. Prozorov, *Effect of Tensile Stress on the In-Plane Resistivity Anisotropy in  $\text{BaFe}_2\text{As}_2$* , *Phys. Rev. B* **85**, 144509 (2012).
- [14] I. R. Shein and A. L. Ivanovskii, *Elastic Properties and Chemical Bonding in Ternary Arsenide  $\text{SrFe}_2\text{As}_2$  and Quaternary Oxyarsenide  $\text{LaFeAsO}$ —Basic Phases for New 38–55 k Superconductors from First Principles*, *Physica (Amsterdam)* **469C**, 15 (2009).
- [15] M. Yoshizawa and S. Simayi, *Anomalous Elastic Behavior and Its Correlation with Superconductivity in Iron-Based Superconductor  $\text{Ba}(\text{Fe}_{1-x}\text{Co}_x)_2\text{As}_2$* , *Mod. Phys. Lett. B* **26**, 1230011 (2012).
- [16] A. Jesche, N. Caroca-Canales, H. Rosner, H. Borrmann, A. Ormeci, D. Kasinathan, H. H. Klauss, H. Luetkens, R. Khasanov, A. Amato, A. Hoser, K. Kaneko, C. Krellner, and C. Geibel, *Strong Coupling between Magnetic and Structural Order Parameters in  $\text{SrFe}_2\text{As}_2$* , *Phys. Rev. B* **78**, 180504 (2008).
- [17] Y. Xiao, Y. Su, M. Meven, R. Mittal, C. M. N. Kumar, T. Chatterji, S. Price, J. Persson, N. Kumar, S. K. Dhar, A. Thamizhavel, and Th. Brueckel, *Magnetic Structure of  $\text{EuFe}_2\text{As}_2$  Determined by Single-Crystal Neutron Diffraction*, *Phys. Rev. B* **80**, 174424 (2009).
- [18] See Supplemental Material at <http://link.aps.org/supplemental/10.1103/PhysRevX.8.011011> for further details of the model and its solution, a detailed phase diagram and energy differences, as well as the description of computational and experimental methodologies, a discussion of possible bilinear interactions, allowed by symmetry in the system, and for a compendium of the domain population data extracted from different samples and by different measurement techniques. A movie illustrating the magnetically induced domain dynamics in  $\text{EuFe}_2\text{As}_2$  is also included.
- [19] S. Jiang, Y. Luo, Z. Ren, Z. Zhu, C. Wang, X. Xu, Q. Tao, G. Cao, and Z. Xu, *Metamagnetic Transition in  $\text{EuFe}_2\text{As}_2$  Single Crystals*, *New J. Phys.* **11**, 025007 (2009).
- [20] J. K. Glasbrenner, I. Žutić, and I. I. Mazin, *Theory of Mn-Doped II-II-V Semiconductors*, *Phys. Rev. B* **90**, 140403(R) (2014).
- [21] C. Yasuda, S. Todo, K. Hukushima, F. Alet, M. Keller, M. Troyer, and H. Takayama, *Néel Temperature of Quasi-Low-Dimensional Heisenberg Antiferromagnets*, *Phys. Rev. Lett.* **94**, 217201 (2005).
- [22] V. Yu. Irkhin and A. A. Katanin, *Thermodynamics of Isotropic and Anisotropic Layered Magnets: Renormalization-Group Approach and  $1/n$  Expansion*, *Phys. Rev. B* **57**, 379 (1998).
- [23] V. Yu. Irkhin and A. A. Katanin, *Report on the Moscow International Symposium on Magnetism*, [arXiv:cond-mat/0001032](https://arxiv.org/abs/cond-mat/0001032).
- [24] J. K. Glasbrenner, I. I. Mazin, Harald O. Jeschke, P. J. Hirschfeld, R. M. Fernandes, and Roser Valentí, *Effect of Magnetic Frustration on Nematicity and Superconductivity in Iron Chalcogenides*, *Nat. Phys.* **11**, 953 (2015).
- [25] Eckhard Limpert, Werner A. Stahel, and Markus Abbt, *Log-Normal Distributions across the Sciences: Keys and Clues*, *BioScience* **51**, 341 (2001).
- [26] K. J. Kurzydowski and B. Ralph, *The Quantitative Description of the Microstructure of Materials* (CRC Press, Boca Raton, 1995).
- [27] J. Maiwald, Y. Xiao, and S. Nandi (to be published).